

Polarization-induced hole doping in N-polar III-nitride LED grown by metalorganic chemical vapor deposition

Long Yan, Yuantao Zhang, Xu Han, Gaoqiang Deng, Pengchong Li, Ye Yu, Liang Chen, Xiaohang Li, and Junfeng Song

Citation: [Appl. Phys. Lett.](#) **112**, 182104 (2018); doi: 10.1063/1.5023521

View online: <https://doi.org/10.1063/1.5023521>

View Table of Contents: <http://aip.scitation.org/toc/apl/112/18>

Published by the [American Institute of Physics](#)

PHYSICS TODAY

WHITEPAPERS

MANAGER'S GUIDE

Accelerate R&D with
Multiphysics Simulation

READ NOW

PRESENTED BY

 **COMSOL**

Polarization-induced hole doping in N-polar III-nitride LED grown by metalorganic chemical vapor deposition

Long Yan,¹ Yuantao Zhang,^{1,a)} Xu Han,¹ Gaoqiang Deng,¹ Pengchong Li,¹ Ye Yu,¹ Liang Chen,¹ Xiaohang Li,² and Junfeng Song¹

¹State Key Laboratory of Integrated Optoelectronics, College of Electronic Science and Engineering, Jilin University, Qianjin Street 2699, Changchun 130012, China

²King Abdullah University of Science and Technology (KAUST), Advanced Semiconductor Laboratory, Thuwal 23955-6900, Saudi Arabia

(Received 25 January 2018; accepted 23 April 2018; published online 3 May 2018)

Polarization-induced doping has been shown to be effective for wide-bandgap III-nitrides. In this work, we demonstrated a significantly enhanced hole concentration via linearly grading an N-polar $\text{Al}_x\text{Ga}_{1-x}\text{N}$ ($x = 0\text{--}0.3$) layer grown by metal-organic chemical vapor deposition. The hole concentration increased by ~ 17 times compared to that of N-polar p-GaN at 300 K. The fitting results of temperature-dependent hole concentration indicated that the holes in the graded p-AlGaN layer comprised both polarization-induced and thermally activated ones. By optimizing the growth conditions, the hole concentration was further increased to $9.0 \times 10^{17} \text{ cm}^{-3}$ in the graded AlGaN layer. The N-polar blue-violet light-emitting device with the graded p-AlGaN shows stronger electroluminescence than the one with the conventional p-GaN. The study indicates the potential of the polarization doping technique in high-performance N-polar light-emitting devices. *Published by AIP Publishing.* <https://doi.org/10.1063/1.5023521>

GaN and AlN and their ternary alloys have a direct bandgap ranging from 3.4 (GaN) to 6.2 eV (AlN). Because of their large bandgap, they are widely used in the fabrication of ultraviolet (UV) devices such as UV light-emitting diodes (LEDs), laser diodes, and UV solar blind detectors.^{1–3} However, the low conductivity in the p-type AlGaN layer has hindered the development of high efficiency and output power devices largely due to the high activation energy of the Mg acceptor, which is ~ 150 meV in GaN and increases monotonically with the Al content in AlGaN.⁴ This means a very small percentage of acceptor ionization (less than 0.5%) in AlGaN at room temperature.

Recently, polarization-induced hole doping has been demonstrated as a feasible approach to increasing the ionization probability of the Mg acceptor. Negative bound unbalanced charges can be created in a compositionally graded AlGaN layer because of different magnitudes of the polarization in AlGaN with different Al contents. Then the holes are field-ionized from the Mg acceptors to neutralize the negative bound polarization charges. The holes generated by this method have a high density with a weak temperature dependence.⁵ Up to now, this method has been used to realize p-type doping in metal- and N-polar AlGaN by molecular beam epitaxy (MBE) and metal-polar AlGaN by metal-organic chemical vapor deposition (MOCVD).^{5–7} The N-polar GaN-based structures grown by MOCVD have typically high background electron concentration.⁸ Few works have been reported on achieving p-type conduction in N-polar AlGaN by MOCVD. In our previous work,⁹ we reduced the background electron concentration of N-polar GaN by optimizing the V/III ratio. Based on this optimization, we achieved N-polar p-type AlGaN by using the

polarization-induced doping method with the MOCVD technique. Moreover, in previous works on polarization doping, the measured hole concentrations always show a slight rise with increasing temperature, but the authors failed to offer any clear explanation. In this work, we proposed a model to explain the difference between the simulated polarization charge density and the measured hole concentration.

The samples used in this study were grown on sapphire substrates by using an AIXTRON CCS 3×2 " FT MOCVD system. Triethylgallium (TEGa), trimethylgallium (TMGa), trimethylaluminum (TMAI), and high-purity ammonia (NH_3) were used as the source precursors for Ga, Al, and N, respectively. Bis-cyclopentadienyl magnesium (Cp_2Mg) was employed as the p-type dopant. First, a $2\text{-}\mu\text{m}$ -thick N-polar GaN template was initially grown on sapphire substrates, and the detailed growth conditions can be found in our previous study.¹⁰ Then, an $\sim 75\text{-nm}$ -thick Mg-doped AlGaN layer with the Al content linearly graded from 0 to 0.3 was grown on the template at 1020°C . To realize the graded Al content, the TMAI flow rate was increased linearly from 0 to $15 \mu\text{mol/min}$, and the TMGa flow rate was decreased linearly from 50 to $35 \mu\text{mol/min}$ during the growth process. Meanwhile, the Cp_2Mg and NH_3 flow rates were kept at 60 nmol/min and $2.2 \times 10^5 \mu\text{mol/min}$, respectively. Finally, the as-grown sample was annealed at 720°C in a nitrogen ambient to activate the Mg acceptor. For comparison, we prepared another reference sample, where a 100-nm -thick Mg-doped GaN layer with the same growth conditions of the Mg-doped AlGaN layer was grown on the $2\text{-}\mu\text{m}$ -thick N-polar GaN template as we mentioned above. The Al content and strain were examined using an X-ray diffractometer (XRD; Rigaku Ultima IV). The electrical properties were investigated by Hall effect measurements (ACCENT HL5500PC, UK). The Ohmic contacts were realized by

^{a)}E-mail: zhangyt@jlu.edu.cn

depositing Ni/Au metal layers using a rapid thermal annealing process.

To check the Al content distribution, the XRD 2θ - ω scan was conducted and simulated around the $(10\bar{1}5)$ peak of GaN and AlGaIn, as shown in Fig. 1(a). The stronger peak located in 105.5° belongs to the GaN template. The broad and flat shoulder peak near the GaN peak is from AlGaIn, which means that the linearly graded distribution of the Al content in the AlGaIn layer is formed. The close match between the measured and the simulated data indicates that the component and the thickness of the graded AlGaIn layer can be accurately controlled by the MOCVD process. To further confirm the linear distribution of the Al content in the AlGaIn layer, XRD reciprocal space mapping (RSM) measurements were performed and the results are shown in Fig. 1(b). According to the tail profile above the reciprocal space lattice point of GaN, we can confirm that the Al content has a linear distribution in AlGaIn, which is consistent with the 2θ - ω scanning measurement result. At the same time, the overlap between the tail profile and the fully strained line (the dotted pink line) means that there is no tensile strain relaxation in the graded AlGaIn layer. When AlGaIn is in the tensile strain state, the direction of piezoelectric polarization is the same as that of spontaneous polarization.¹¹ In the fully strained graded AlGaIn layer, the magnitude of piezoelectric polarization increases with the increasing Al content, which

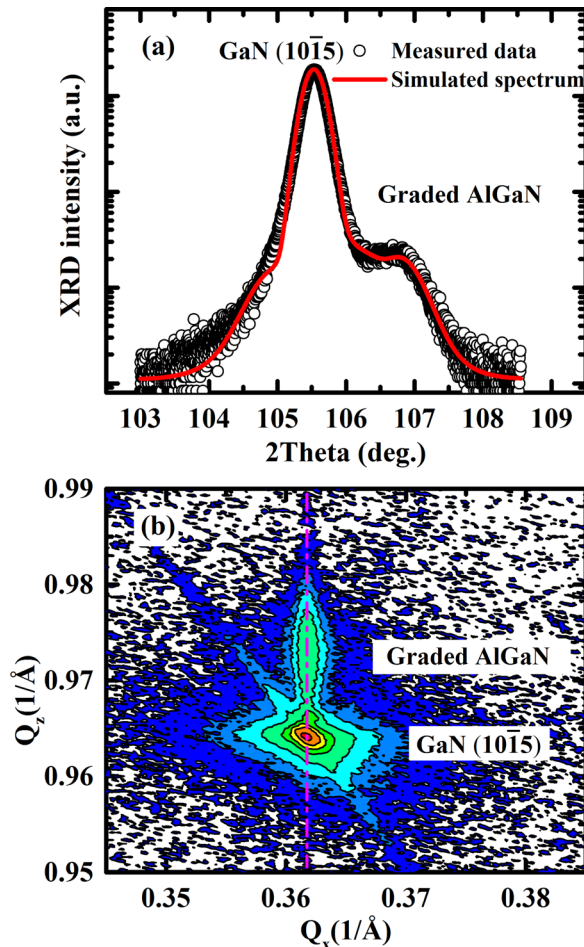


FIG. 1. X-ray diffraction spectrum (a) and reciprocal space map (b) of the $(10\bar{1}5)$ reflection plane for the graded AlGaIn on the GaN template.

is the same as the trend of spontaneous polarization. Therefore, the fully strained state in the graded AlGaIn layer can further increase the polarization gradient.

Based on the distribution of the Al content and the stress state in the graded AlGaIn, we can estimate the density of polarization charge, which is created by the difference in polarization in the graded AlGaIn, through the formula $\rho_\pi(z) = \nabla P(z)$, where ∇ is the divergence operator and $P(z)$ is the sum of spontaneous and piezoelectric polarizations. If the Al content is small enough, a simple linear model may be used to calculate the polarization charge density of AlGaIn,⁵ which is given by $5 \times 10^{13} \times (x/d) \text{ cm}^{-3}$, where x is the Al content at the ended interference of the graded AlGaIn and d is the thickness of the graded layer. Therefore, the density of the polarization charges in our graded AlGaIn layer may be as high as $2 \times 10^{18} \text{ cm}^{-3}$. In theory, the field-ionized free holes have the same concentration with the polarization charge.

To probe the hole concentration and verify the acceptor-activation method, temperature dependent Hall measurements were carried out on both the graded p-AlGaIn and the reference sample (p-GaN). The results are shown in Fig. 2(a). The hole concentration of the graded p-AlGaIn layer is $6.4 \times 10^{17} \text{ cm}^{-3}$ at 300 K, which is ~ 17 times higher than that of the p-GaN layer ($3.7 \times 10^{16} \text{ cm}^{-3}$). As the temperature decreases from 450 to 150 K, the hole concentration in the p-GaN layer (the green triangles) decreases exponentially, which is the typical freezeout phenomenon for thermally activated holes. However, the hole concentration of the graded AlGaIn layer (the blue squares) shows a weak temperature dependence. The absence of freezeout in the graded AlGaIn layer reveals that the holes in the graded AlGaIn layer are mainly created by the polarization electric field. Besides, it is worth noting that the measured hole concentration of the graded AlGaIn layer is lower than the density of polarization charge (the gray solid line). Meanwhile, when the temperature is higher than 250 K, the hole concentration shows a slight rise with increasing temperature. This behavior is similar to the freezeout phenomenon from thermally activated holes. Hence, we speculate that the holes in the graded AlGaIn layer include both field-ionized holes and thermally activated holes. When the temperature is low

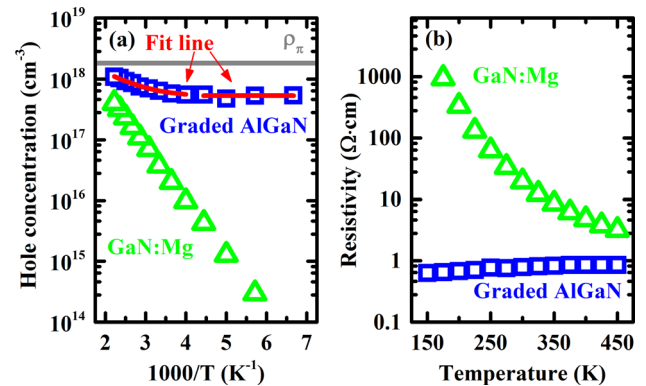


FIG. 2. Temperature dependent hole concentration (a) and resistivity (b) of the graded p-AlGaIn and the p-GaN. The gray line indicates the concentration of polarization-induced volume charges predicted by the theory. The red line is the fitting result using Eq. (1).

enough, such as 150 K to 225 K, the thermally activated holes are relatively sparse. The measured hole concentration of the graded AlGaIn layer is similar to the concentration of field-ionized holes, which is temperature-independent. When the temperature further goes up, the thermally activated hole concentration gets close to the field-ionized hole concentration. As a consequence, the measured hole concentration is affected by the thermally activated hole, which is proportional to the temperature. In this situation, the concentration of the measured holes can be expressed by

$$p = p_0 + p_\pi = N_A - N_D - p_A, \quad (1)$$

where p_0 is the concentration of thermally activated holes, p_π is the concentration of field-ionized holes which is equal to the density of polarization charge, N_A is the acceptor concentration, N_D is the compensating donor concentration, and p_A is the inactivated acceptor concentration. To verify this inference, the measured hole-concentration data are fitted in two different temperature ranges. When the temperature is lower than 225 K, we only consider the field-ionized holes. However, when the temperature is higher than 250 K, the temperature-dependent hole concentrations are fitted by Eq. (2) as follows, which combines Eq. (1) with the single-acceptor model and Boltzmann statistics:

$$\frac{p_0(p_0 + p_\pi + N_D)}{N_A - N_D - p_0 - p_\pi} = \frac{N_V}{g} \exp\left(-\frac{E_A}{k_B T}\right), \quad (2)$$

where N_V is the effective density of states in the valence band $[2(2\pi m_h^* k_B T)^{3/2}/h^3]$, g is the acceptor degeneracy factor (4 for GaN),¹² E_A is the acceptor activation energy, k_B is the Boltzmann constant, and T is the absolute temperature. The good agreement between the model predictions (the red solid lines) and the measured hole concentrations in the entire temperature range verifies the assumed model. However, according to the fitted results, the polarization charge density in our samples is only $\sim 30\%$ of the calculated one. We speculate that it can be attributed to the screening effect caused by defects. However, further investigations are needed to demonstrate it. Besides, temperature dependent resistivities of the p-GaN layer and the graded p-AlGaIn layer were also measured, and the results are shown in Fig. 2(b). The resistivity of the graded AlGaIn layer is $\sim 0.8 \Omega \text{ cm}$ at 300 K, which is far less than that of the p-GaN layer ($\sim 19.6 \Omega \text{ cm}$). As the temperature increases from 150 K to 450 K, the resistivity of the p-GaN layer decreases by more than two orders of magnitude. In contrast, the resistivity of the graded p-AlGaIn layer shows a slow increase with increasing temperature. Our result is very similar to that reported in Ref. 5, in which the authors attributed this metal-like behavior to the absence of hole freezeout and the decrease in mobility with the increase in temperature.

According to the above fitting results, we can know that the hole concentration of the graded AlGaIn can be improved by decreasing the compensation donors or increasing the acceptors. In our previous study,¹⁰ we proved that an *in-situ* SiN_x mask in N-polar GaN can decrease the concentration of oxygen donors. Therefore, we also inserted a SiN_x mask in the N-polar GaN template during the growth interruption

TABLE I. The list of hole concentrations for the graded AlGaIn with and without the SiN_x mask depending on different Cp₂Mg flow rates.

SiN _x mask	Cp ₂ Mg flow (nmol/min)	Hole concentration ($\times 10^{17} \text{ cm}^{-3}$)
w/o	60	6.4
W	50	7.0
W	60	7.9
W	70	9.0
W	80	7.9

after the growth of 300-nm-thick GaN. Meanwhile, the growth conditions for the graded AlGaIn on the GaN template remain unchanged. The hole concentrations measured by Hall measurements at 300 K are listed in Table I. The result shows that the hole concentration in the graded AlGaIn increases from 6.4×10^{17} to $7.9 \times 10^{17} \text{ cm}^{-3}$ by inserting the SiN_x mask. Then, we optimized the flow rate of Cp₂Mg during the graded AlGaIn growth. We find that the largest hole concentration of $9.0 \times 10^{17} \text{ cm}^{-3}$ is obtained in the graded AlGaIn layer when the Cp₂Mg flow rate is 70 nmol/min.

Furthermore, to confirm the benefits of having the graded AlGaIn layer for optical devices, InGaIn/GaN multiple-quantum-well (MQW) LEDs with the graded p-AlGaIn

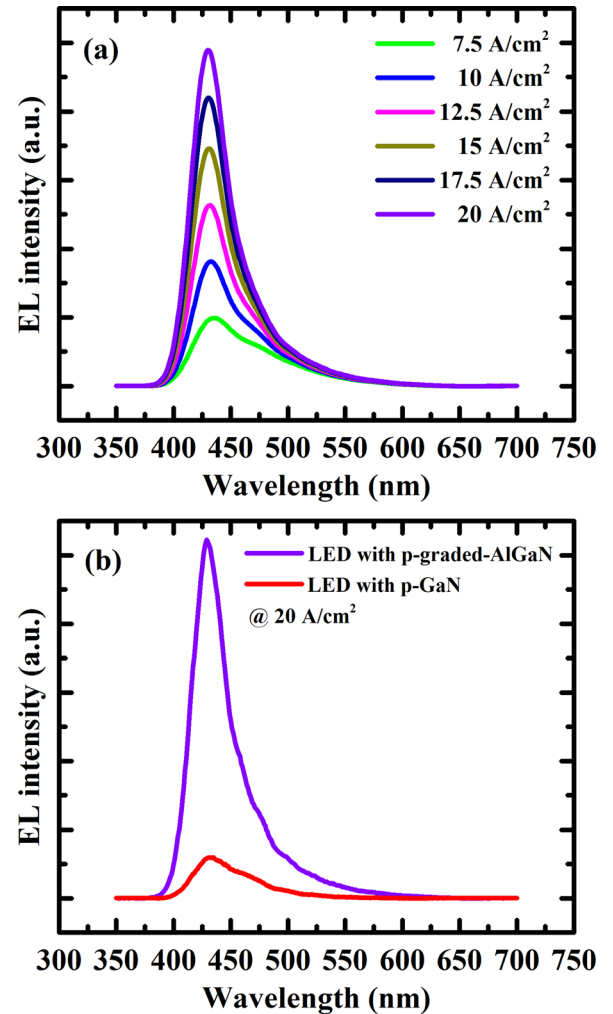


FIG. 3. (a) EL spectra of the LED with graded p-AlGaIn at various injection current densities (ranging from 7.5 A/cm^2 to 20 A/cm^2). (b) EL spectra of the LEDs with p-GaN and graded p-AlGaIn at 20 A/cm^2 .

layer and the p-GaN layer were grown by MOCVD, respectively. The epitaxial structure of our LED samples includes a 500-nm-thick n-type GaN grown on the 2- μ m-thick N-polar GaN template, followed by 5 pairs of MQWs and the graded p-AlGaIn layer or the p-GaN layer. The growth conditions of the graded p-AlGaIn layer and the p-GaN layer are same as those of the optimized samples mentioned above. The EL spectra of the LED with the graded p-AlGaIn layer at different driving current densities (ranging from 7.5 to 20 A/cm²) are shown in Fig. 3(a). The emission peak wavelength shifts from 435 nm at 7.5 A/cm² to 430 nm at 20 A/cm². The slight blue-shift of the emission peak with the increase in injection current can be attributed to the free-carrier screening effect on the polarization field in MQWs.¹³ Figure 3(b) shows the EL spectra of the two LED samples at 20 A/cm². We can see that the peak wavelength of the LED with p-GaN is the same as that of the LED with graded p-AlGaIn. Besides, it can be observed obviously that the EL intensity of the LED with graded p-AlGaIn is significantly higher than that of the LED with p-GaN due to the higher hole concentration of the graded p-AlGaIn.

In conclusion, we demonstrated effective polarization-induced hole doping via compositionally linearly graded N-polar Al_xGa_{1-x}N (x = 0–0.3) grown by MOCVD. The XRD results show that the component and the thickness of the graded AlGaIn layer can be accurately controlled by the MOCVD growth process. The absence of the hole-freezeout-effect at low temperature indicates that the holes are mainly induced by polarization charges. The increase in the hole concentration at high temperature can be attributed to the thermally activated holes. Besides, we increase the hole concentration of the graded AlGaIn layer from 6.9×10^{17} to 9.0×10^{17} cm⁻³ by optimizing the growth conditions. The stronger EL intensity of the N-polar blue-violet LED with the graded p-AlGaIn, compared to the N-polar

LED with the conventional p-GaN, indicates the great potential of the polarization-induced doping in N-polar III-nitride light-emitting devices.

This work was supported by the National Key Research and Development Program (No. 2016YFB0400103), the National Natural Science Foundation of China (Nos. 61674068 and 61734001), and the Science and Technology Developing Project of Jilin Province (20150519004JH, 20160101309JC, and 20170204045GX).

- ¹A. A. Allerman, M. H. Crawford, A. J. Fischer, K. H. A. Bogart, S. R. Lee, D. M. Follstaedt, P. P. Provencio, and D. D. Koleske, *J. Cryst. Growth* **272**(1–4), 227 (2004).
- ²H. Yoshida, Y. Yamashita, M. Kuwabara, and H. Kan, *Appl. Phys. Lett.* **93**(24), 241106 (2008).
- ³G. Bao, D. Li, X. Sun, M. Jiang, Z. Li, H. Song, H. Jiang, Y. Chen, G. Miao, and Z. Zhang, *Opt Express* **22**(20), 24286 (2014).
- ⁴J. Li, T. N. Oder, M. L. Nakarmi, J. Y. Lin, and H. X. Jiang, *Appl. Phys. Lett.* **80**(7), 1210 (2002).
- ⁵J. Simon, V. Protasenko, C. Lian, H. Xing, and D. Jena, *Science* **327**(5961), 60 (2010).
- ⁶S. B. Li, T. Zhang, J. Wu, Y. J. Yang, Z. M. Wang, Z. M. Wu, Z. Chen, and Y. D. Jiang, *Appl. Phys. Lett.* **102**(6), 062108 (2013).
- ⁷L. Zhang, K. Ding, J. C. Yan, J. X. Wang, Y. P. Zeng, T. B. Wei, Y. Y. Li, B. J. Sun, R. F. Duan, and J. M. Li, *Appl. Phys. Lett.* **97**(6), 062103 (2010).
- ⁸M. Sumiya, K. Yoshimura, K. Ohtsuka, and S. Fuke, *Appl. Phys. Lett.* **76**(15), 2098 (2000).
- ⁹J. Y. Jiang, Y. T. Zhang, F. Yang, Z. Huang, L. Yan, P. C. Li, C. Chi, D. Q. Zhao, B. L. Zhang, and G. T. Du, *Vacuum* **119**, 63 (2015).
- ¹⁰L. Yan, Y. T. Zhang, H. Xu, L. Li, J. Y. Jiang, Z. Huang, X. Han, J. F. Song, and G. T. Du, *Mater. Sci. Semicond. Process.* **59**, 35 (2017).
- ¹¹O. Ambacher, J. Smart, J. R. Shealy, N. G. Weimann, K. Chu, M. Murphy, W. J. Schaff, L. F. Eastman, R. Dimitrov, L. Wittmer, M. Stutzmann, W. Rieger, and J. Hilsenbeck, *J. Appl. Phys.* **85**(6), 3222 (1999).
- ¹²H. Okumura, D. Martin, M. Malinverni, and N. Grandjean, *Appl. Phys. Lett.* **108**(7), 072102 (2016).
- ¹³F. Della Sala, A. Di Carlo, P. Lugli, F. Bernardini, V. Fiorentini, R. Scholz, and J. M. Jancu, *Appl. Phys. Lett.* **74**(14), 2002 (1999).